

62
1960

DETERMINATION OF ROTATIONAL AND RADIAL COMPONENTS
OF INDUCED VELOCITY FOR A TWO-BLADED ROTOR
HOVERING IN GROUND EFFECT

A THESIS

Presented to
the Faculty of the Graduate Division

by
Adalbert Edward Toepel, Jr.

In Partial Fulfillment
of the Requirements for the Degree
Master of Science in Aeronautical Engineering

Georgia Institute of Technology

June, 1960

DETERMINATION OF ROTATIONAL AND RADIAL COMPONENTS
OF INDUCED VELOCITY FOR A TWO-BLADED ROTOR
HOVERING IN GROUND EFFECT

Approved:

Walter Castles, Jr. ²/₄

Robin B. Gray

Thomas W. Jackson

Date approved by Chairman: May 31, 1960

ACKNOWLEDGMENTS

The author wishes to express his appreciation to Professor Walter Castles, Jr., for the suggestion of the topic and for his valuable guidance throughout the preparation of this thesis. Gratitude is also extended to Doctor Robin B. Gray and Doctor Thomas W. Jackson for their review and comments on the material contained herein.

TABLE OF CONTENTS

	Page
ACKNOWLEDGMENTS.	ii
LIST OF FIGURES.	iv
LIST OF SYMBOLS.	v
SUMMARY.	vii
Chapter	
I. INTRODUCTION.	1
II. APPARATUS AND EXPERIMENTAL PROCEDURE.	3
III. RESULTS	9
IV. APPLICATION OF RESULTS.	10
V. CONCLUDING REMARKS.	15
FIGURES.	16
BIBLIOGRAPHY	29

LIST OF FIGURES

Figure	Page
1. Diagram of Primary Circuit	16
2. Vortex System Model.	17
3. Search Coil Assembly	18
4. Normalizing Coil	19
5. Amplifier and Output Meter	20
6. Nondimensional Rotational Components of Induced Velocity at Various Nondimensional Heights	
(a) For an Azimuth Angle of 5 Degrees Behind the Rotor Blade.	21
(b) For an Azimuth Angle of 50 Degrees Behind the Rotor Blade.	22
(c) For an Azimuth Angle of 95 Degrees Behind the Rotor Blade.	23
(d) For an Azimuth Angle of 140 Degrees Behind the Rotor Blade.	24
7. Nondimensional Radial Components of Induced Velocity at Various Nondimensional Heights	
(a) For an Azimuth Angle of 5 Degrees Behind the Rotor Blade.	25
(b) For an Azimuth Angle of 50 Degrees Behind the Rotor Blade.	26
(c) For an Azimuth Angle of 95 Degrees Behind the Rotor Blade.	27
(d) For an Azimuth Angle of 140 Degrees Behind the Rotor Blade.	28

LIST OF SYMBOLS

A	rotor disc area
b	number of rotor blades
C_T	rotor thrust coefficient, $C_T = T/\rho\pi\Omega^2R^4$
M	moment
MR	meter reading, decibels
N	subscript for a value at the normalizing point
n	number of turns of wire on the reference coil
P	subscript for a value at an arbitrary point P
q	dynamic pressure, $q = \frac{1}{2} \rho V^2$
R	rotor radius
R_c	radius of reference coil
R_m	wire model rotor radius
r	distance to an arbitrary point on the rotor disc from the axis
T	rotor thrust
V	resultant velocity
v_n	normal component of induced velocity
v_r	radial component of induced velocity
v_t	rotational component of induced velocity
W	weight of the helicopter
z	distance to an arbitrary point from the ground plane in a direction normal to the ground plane

Γ	vortex strength
α	angle of attack of a blade element
ϕ	induced angle of attack of a blade element
Θ	blade pitch angle, $\Theta = \alpha + \phi$
ρ	air density
Ω	angular velocity of the rotor

SUMMARY

This experimental investigation was undertaken to determine the rotational and radial components of induced velocity of a two-bladed helicopter rotor hovering at a height of one rotor radius above the ground. An electromagnetic analog in the form of a helical wire model of the wake vortex system was utilized, and measurements were made of the magnetic field intensity at specified points in the flow field about the wire vortex model and its image.

The present work used a model having a wire "vortex system" consisting of the tip vortex pattern, the constant blade bound vortex, and the vortex down the blade axis to the ground plane. Measurements were made of the components of field strength in the tangential and radial directions at five nondimensional heights with respect to the rotor radius-- $z/R = 0.6, 0.8, 1.0, 1.2, \text{ and } 1.4$. Readings were made at azimuth angles 45 degrees apart. The results are presented in nondimensional quantities such that under comparable conditions the velocity can be readily found by knowing the rotor radius and blade bound vortex strength of the two-bladed rotor in question.

The data should be useful for estimating interference induced velocities at the fuselage and tail rotor of two-bladed single rotor helicopters. In addition, the results may be of use for estimating the interference induced velocities at the second rotor of two-bladed twin rotor helicopters.

CHAPTER I

INTRODUCTION

In determining the performance of a lifting rotor, it is necessary to determine the blade angle of attack distribution. In hovering flight the true angle of attack is the blade pitch angle less the induced angle. Accurate determination of the induced angle of attack is difficult, since the local induced velocity has components in the normal, rotational and radial directions with respect to the rotor blade. The assumption that the rotational and radial components are negligible is usually made in order to simplify the determination of the angle of attack distribution. The rotational component affects the angle of attack distribution of the rotor blade. The radial component does not affect the main rotor blade angle of attack, but does affect the tail rotor and the second rotor of a tandem rotor helicopter. In order to determine the magnitude and distribution of these effects, this work was undertaken.

Prior to this work, in reference 1, the wire model of the vortex system from one of the two blades was made from photographs of smoke introduced into the tip vortex. The present work used a model having a wire "vortex system" consisting of the tip vortex pattern, the constant blade bound vortex, and the vortex down the blade axis to the ground plane.

Findings are presented in nondimensional form such that the approximate value of rotational and radial components of induced

velocity distribution may be determined for two-bladed helicopter rotors at or near the flight condition studied.

CHAPTER II

APPARATUS AND EXPERIMENTAL PROCEDURE

The equipment used for the experimental portion of this thesis consisted of the following components:

1. Primary coil (helical wire model of the vortex system).
2. Secondary coil (search coil).
3. Normalizing coil (reference coil).
4. Amplifier and output meter.
5. Power supply.

The equipment used was essentially the same as that used in reference 1, in which the tip vortex only was simulated, the main exception being that the wire model was altered to simulate, in addition, a blade bound vortex and the accompanying vortex extending down the rotor shaft axis. Components were arranged as shown in Figure 1.

The procedure used was to measure the voltage induced in the search coil by the magnetic field which was produced by the alternating current in the wire vortex model. These measurements were then converted into nondimensional induced velocity ratios.

The accuracy of the method used depends on certain considerations, including those as listed in reference 2. These include:

1. Extraneous magnetic fields.
2. Impure wave forms in the primary and search coil leads.
3. Induced effects in the primary and search coil leads.
4. Search coil dimensions and calibration.
5. Primary-coil field distortion.

6. Improper alignment of search coil axis parallel to axis of desired measurement.
7. Difficulty in positioning search coil in all desired points in vortex model due to model configuration.
8. Inaccuracy of model configuration, inasmuch as the last two turns of wire on the model are the result of an extrapolation.

Attempts were made in the experimental portion to minimize the errors due to the sources listed above.

The following is a description of the components utilized in this experiment.

Primary Coil (Vortex Model).--The wire vortex model of the tip vortex system was originally constructed as described in reference 1. It was modified by running the wire from the blade tip position along the simulated blade span, down the model axis to the ground plane, and then directly outward in the ground plane to join a twisted pair of leads at the outer edge of the model, as shown in Figure 2. The presence of the wire running along the base of the model was not a part of the vortex system, and its effect was eliminated in the superposition procedure. The wire vortex model had a simulated rotor radius of six inches located at a height of one rotor radius above the ground plane. Four complete turns of wire were used to represent the tip vortex system of one blade.

Search Coil.--Since the primary-coil field was nonlinear and point measurements were desired, it was necessary that the search coil dimensions be small compared with the dimensions of the vortex model. The search coil, which was the same as that used in reference 1, had

a diameter of approximately 0.35 inches to the center of the wire bundle. The coil consisted of 1,000 turns of No. 40, Brown and Sharpe gage, insulated copper wire wound on a plexiglass coil which was mounted on a plexiglass support. A coaxial cable was used to connect the search coil to the amplifier to eliminate induced voltages in this portion of the circuit. Figure 3 shows the search coil assembly together with its coaxial connector.

Normalizing Coil.--A normalizing, or calibration, coil was placed in series with the vortex model. The coil had a diameter of twelve inches, and consisted of nine turns of No. 17, Brown and Sharpe gage, copper wire wound on a plexiglass ring. The normalizing coil is shown in Figure 4.

Amplifier and Output Meter.--The pickup circuit included a commercial standing wave indicator, in addition to the search coil and coaxial cable. The standing wave indicator had a maximum sensitivity of 0.1 microvolt for full scale deflection, and consisted of an indicating meter, a high-gain 400 cycle fixed-frequency amplifier with a calibrated gain control covering a range of 60 decibels, and a narrow 400 cycle band-pass-filter with a sharp cutoff at 400 ± 5 cycles per second. The input impedance of the amplifier was 200,000 ohms, which was sufficient to eliminate the necessity for any calibration of the meter scale. The amplifier was placed a large distance from the wire vortex model and normalizing coil to eliminate any appreciable magnetic coupling from these coils. The standing wave indicator is shown in Figure 5.

Power Supply.--The power supply consisted of a 400 cycle aircraft alternator driven by a synchronous motor. Components of the circuit included an ammeter, voltmeter, capacitors, and variable resistors.

The capacitance was adjusted by trial and error to approximately tune the circuit to a resonant condition. The resistors were adjusted to limit the current to approximately 3.0 amperes. The power supply was located in a room separate from the vortex model and output meter to reduce magnetic coupling.

Field Survey Procedure.--The primary coil circuit was given a minimum warm-up period of 45 minutes to obtain a stable condition before any measurements were taken. The search coil was then placed in the center of the normalizing coil with the axes of both coils coincident and the meter adjusted to read 30.00 decibels. The search coil was then used to measure the rotational and radial components at each of the five nondimensional rotor heights, $z/R = 0.6, 0.8, 1.0, 1.2, \text{ and } 1.4$. Measurements were taken out to a distance of $1.33R$ at each of eight azimuth angles. Due to the blade bound vortex wire on the present model, it was necessary to take the initial azimuth angle five degrees behind the blade axis. The other seven azimuth angles were spaced 45 degrees apart. The effect of the ground plane was determined by measuring the field strength at corresponding points in the space below the base of the wire vortex model. The search coil was frequently placed in the normalizing coil to verify that there was no appreciable shift in the field strength reference level.

Reduction of Data.--The meter readings recorded for the field survey were in units of decibels, and it was therefore necessary to convert them to a useful form. The following formulas from reference 1 were used:

$$\frac{v_t R}{\Gamma} = \left[\frac{n}{2} \right] \left[\frac{R_m}{R_c} \right] \left[\frac{\text{antilog } 0.1 (MR)_P}{\text{antilog } 0.1 (MR)_N} \right]$$

$$\frac{v_r R}{\Gamma} = \left[\frac{n}{2} \right] \left[\frac{R_m}{R_c} \right] \left[\frac{\text{antilog } 0.1 (MR)_P}{\text{antilog } 0.1 (MR)_N} \right]$$

where

- N subscript referring to normalizing coil
- n number of turns on reference coil
- P subscript referring to the space point at which
the measurement was made
- R rotor radius
- R_c radius of reference coil
- R_m wire model rotor radius
- v_r component of vortex induced velocity in the
radial direction
- v_t component of vortex induced velocity in the
rotational direction.

The sign (or direction) of the induced velocity was determined from vortex geometry and the trends in the experimental data being reduced. The sign convention selected is that rotational velocity components in the same direction as the blade rotation are positive, and that the outward radial velocity components are positive.

Only the vortex model for one of the two blades was used, requiring superposition to obtain the effects of both blades. Readings were taken in all eight azimuth positions, and results from opposite azimuth positions superimposed. This was done for the image also, and

the image results superimposed to give the final solution for both blades.

CHAPTER III

RESULTS

Figure 6 gives the nondimensional rotational component, $v_t R/\Gamma$, of the induced velocity versus nondimensional rotor radius, r/R , for each of the five nondimensional heights, $z/R = 0.6, 0.8, 1.0, 1.2,$ and 1.4 , and eight azimuth angles spaced 45 degrees apart that were selected for measurement.

Figure 7 gives the nondimensional radial component, $v_r R/\Gamma$, of the induced velocity versus nondimensional rotor radius, r/R , for each of the five nondimensional heights, $z/R = 0.6, 0.8, 1.0, 1.2,$ and 1.4 , and eight azimuth angles spaced 45 degrees apart that were selected for measurement.

It should be noted that the results herein presented are strictly applicable only to two-bladed rotors having a vortex system comparable to the simplified configuration of the original vortex system. However, it is believed that the results will remain reasonably valid for values of C_T not too different from that of reference 1, in which $C_T \approx 0.0043$.

CHAPTER IV

APPLICATION OF RESULTS

Determination of Γ .--In order to use the values given on Figures 6 and 7, the nondimensional quantities must be converted to dimensional values. Given the geometry of the helicopter rotor, the assumed constant blade bound vortex strength, Γ , can be obtained as follows:

The thrust, dT , on a blade element is

$$dT = \rho \Gamma \Omega r dr \quad (1)$$

Then the rotor thrust, T , is

$$T = \rho \Gamma \Omega b \int_0^R r dr$$

$$T = \frac{1}{2} \rho \Gamma \Omega b R^2 \quad (2)$$

The rotor thrust coefficient, C_T , is defined as

$$C_T = \frac{T}{\rho \pi \Omega^2 R^4} \quad (3)$$

Substituting Equation (2) into Equation (3),

$$C_T = \frac{1}{2} \frac{\rho \Gamma \Omega b R^2}{\rho \pi \Omega^2 R^4} = \frac{\Gamma b}{2 \pi \Omega R^2} \quad (4)$$

Rearranging,

$$\Gamma = \frac{2 \pi \Omega R^2 C_T}{b} \quad (5)$$

Equation (5) can now be used to obtain the blade bound vortex strength, permitting evaluation of rotational and radial components of induced velocity.

Sample Application.--A possible use for the data on the rotational component of induced velocity would be the determination of forces on the fuselage of a single rotor helicopter in hovering flight. Due to the long moment arm of the fuselage for side forces acting near the tail rotor, a small force results in an appreciable moment about the center of gravity of the helicopter. Consider, for example, the Bell model 47J helicopter. A point on the fuselage at a distance of $0.9R$ from the rotor hub is 190 inches from the rotor shaft axis and $0.2R$ below the plane of the rotor. The nondimensional values for the rotational component of induced velocity for this point on the fuselage, as extracted from Figure 6, are:

$$\frac{v_t R}{\Gamma} = 0.87, 0.22, 0.09, \text{ and } 0.12$$

The average of these values is

$$\left(\frac{v_t R}{\Gamma} \right)_{\text{average}} = 0.33$$

For solution of this problem, the following data are assumed:

$T \approx W = 2,450$ pounds	$A = 969$ square feet
$\rho = 0.002378$ slugs/cubic foot	$R = 17.56$ feet
$\Omega = 36.07$ radians/second	
$\Omega R = 633.5$ feet/second	
$b = 2$ blades	

Then the solution for the thrust coefficient, C_T , yields

$$C_T = \frac{T}{\rho(\Omega R)^2 A} = \frac{2,450}{(0.002378)(633.5)^2(969)} = 0.00265$$

Vortex strength is next found

$$\begin{aligned} \Gamma &= \frac{2\pi\Omega R^2 C_T}{b} = \frac{2\pi(36.07)(17.56)^2(0.00265)}{2} \\ &= 92.5 \text{ feet}^2/\text{second} \end{aligned}$$

Then

$$\begin{aligned} v_{t \text{ average}} &= (\Gamma/R)(0.33) = (92.5/17.56)(0.33) \\ &= 1.74 \text{ feet/second} \end{aligned}$$

The rotational component of induced velocity, together with the normal component of induced velocity, give a resultant velocity, V , which can be converted to a dynamic pressure, q , on the fuselage of the helicopter. The normal component of induced velocity, for the purposes of this study, will be found by the following approximation:

$$\begin{aligned} v_n/\Omega R &= \sqrt{1/2 C_T} \\ v_n &= \Omega R \sqrt{1/2 C_T} \\ &= 633.5 \sqrt{1/2(0.00265)} \\ &= 23.02 \text{ feet/second} \end{aligned}$$

The resultant velocity, V , is next computed

$$\begin{aligned} V^2 &= \sqrt{v_n^2 + v_t^2} = \sqrt{(23.02)^2 + (1.74)^2} \\ V &= 23.08 \text{ feet/second} \end{aligned}$$

Converting the resultant induced velocity into a dynamic pressure, q , where

$$\begin{aligned} q &= 1/2 \rho V^2 \\ &= 1/2 (0.002378) (23.08)^2 \\ &= 0.633 \text{ pounds/square foot} \end{aligned}$$

The moment about the center of gravity of the helicopter due to this incremental force is, for a drag coefficient of one based on projected area,

$$\begin{aligned} M &= (\text{force})(\text{distance to center of gravity}) \\ &= (0.633)(15.83) \\ &= 10.0 \text{ foot-pounds/square foot of projected area} \end{aligned}$$

The angle of application of this moment with respect to the rotor plane may be found as follows:

$$\begin{aligned} \text{Angle from horizontal plane} &= \tan^{-1} \left(\frac{v_n}{v_t} \right) \\ &= \tan^{-1}(23.02/1.74) \\ &= 85.7 \text{ degrees} \end{aligned}$$

Sample Application.--The magnitude of the rotational and radial components of induced velocity at the hub of the tail rotor will next be examined for magnitude. Location of the tail rotor hub is approximately $r/R = 1.2$ and $z/R = 1.0$. The following average values are extracted from Figures 6 and 7:

$$v_t R/\Gamma = 0.149$$

$$v_r R/\Gamma = 0.458$$

Converting to dimensional quantities,

$$\begin{aligned}v_{t_{\text{average}}} &= (\Gamma/R)(0.149) = (92.5/17.56)(0.149) \\ &= 0.785 \text{ feet/second}\end{aligned}$$

$$\begin{aligned}v_{r_{\text{average}}} &= (\Gamma/R)(0.458) = (92.5/17.56)(0.458) \\ &= 2.415 \text{ feet/second}\end{aligned}$$

Observing the sign conventions, these values would be added to the calculated self-induced velocities at the tail rotor hub to give the total estimated velocities acting at that point.

CHAPTER V

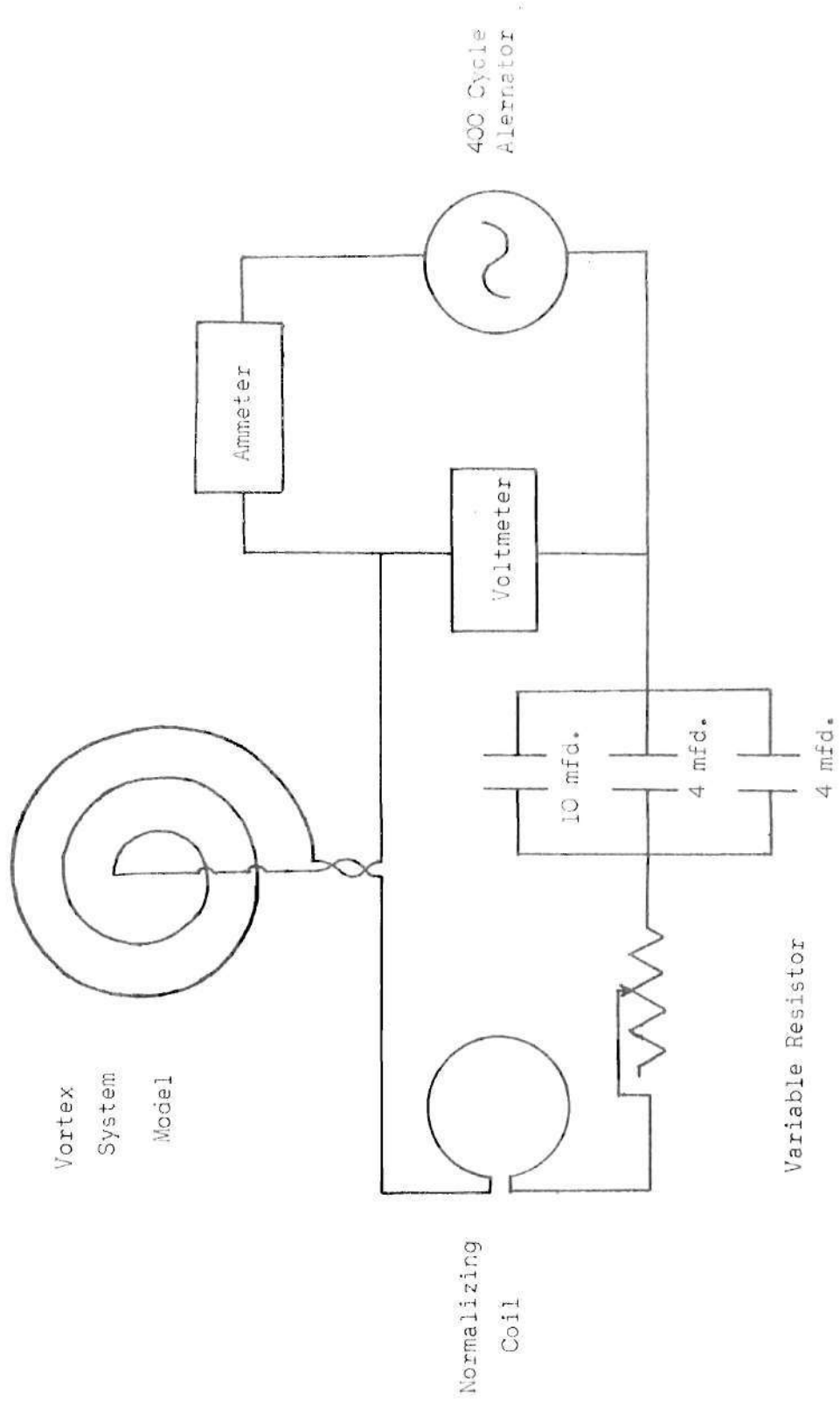
CONCLUDING REMARKS

The accuracy of the experimental data contained in this thesis is not known. However, it is believed that the accuracy is sufficient for most engineering purposes, such as estimating interference induced velocities on the fuselage and tail rotor of a two-bladed single rotor helicopter hovering in ground effect.

The experimental data contained in Figures 6 and 7 may be applied by first determining the circulation strength for a given two-bladed rotor. This can normally be done by use of Equation (5).

The magnitudes of the resulting components of induced velocity are dependent upon the helicopter being examined. The rotor of a large helicopter having a relatively low blade angular velocity would have a higher blade bound vortex strength, and, consequently, higher rotational and radial induced velocity components than would be the case for the rotor of a lighter helicopter with a high rotor angular velocity such as that considered in the sample calculations.

In so far as the actual vortex system corresponds to the simplified configuration of the original vortex system, the data in this paper give the designer necessary information to estimate the magnitudes of the rotational and radial induced velocity components, and thus their relative importance for any particular two-bladed helicopter hovering in ground effect.



Capacitors

Figure 1. Diagram of Primary Circuit

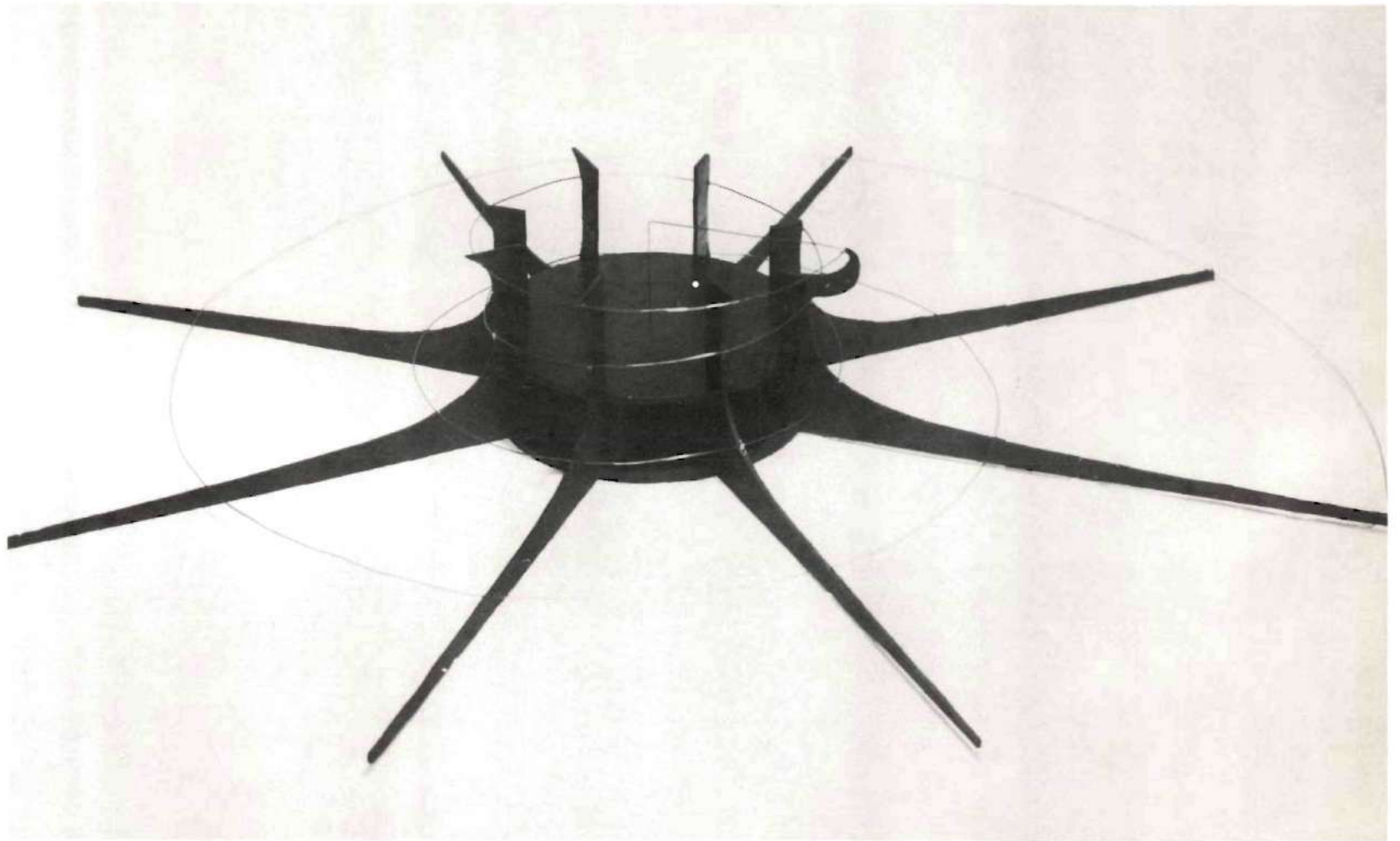


Figure 2. Vortex System Model

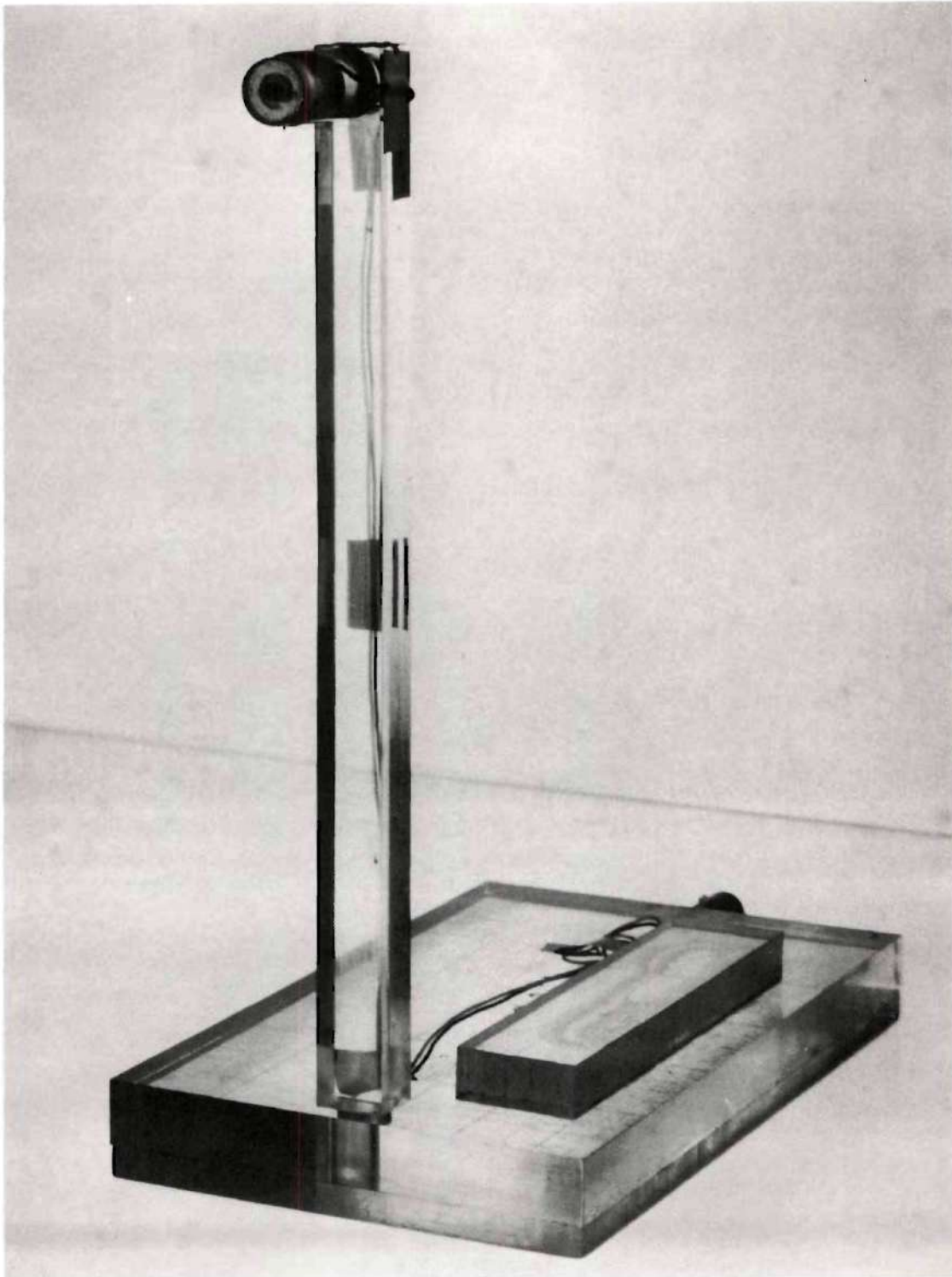


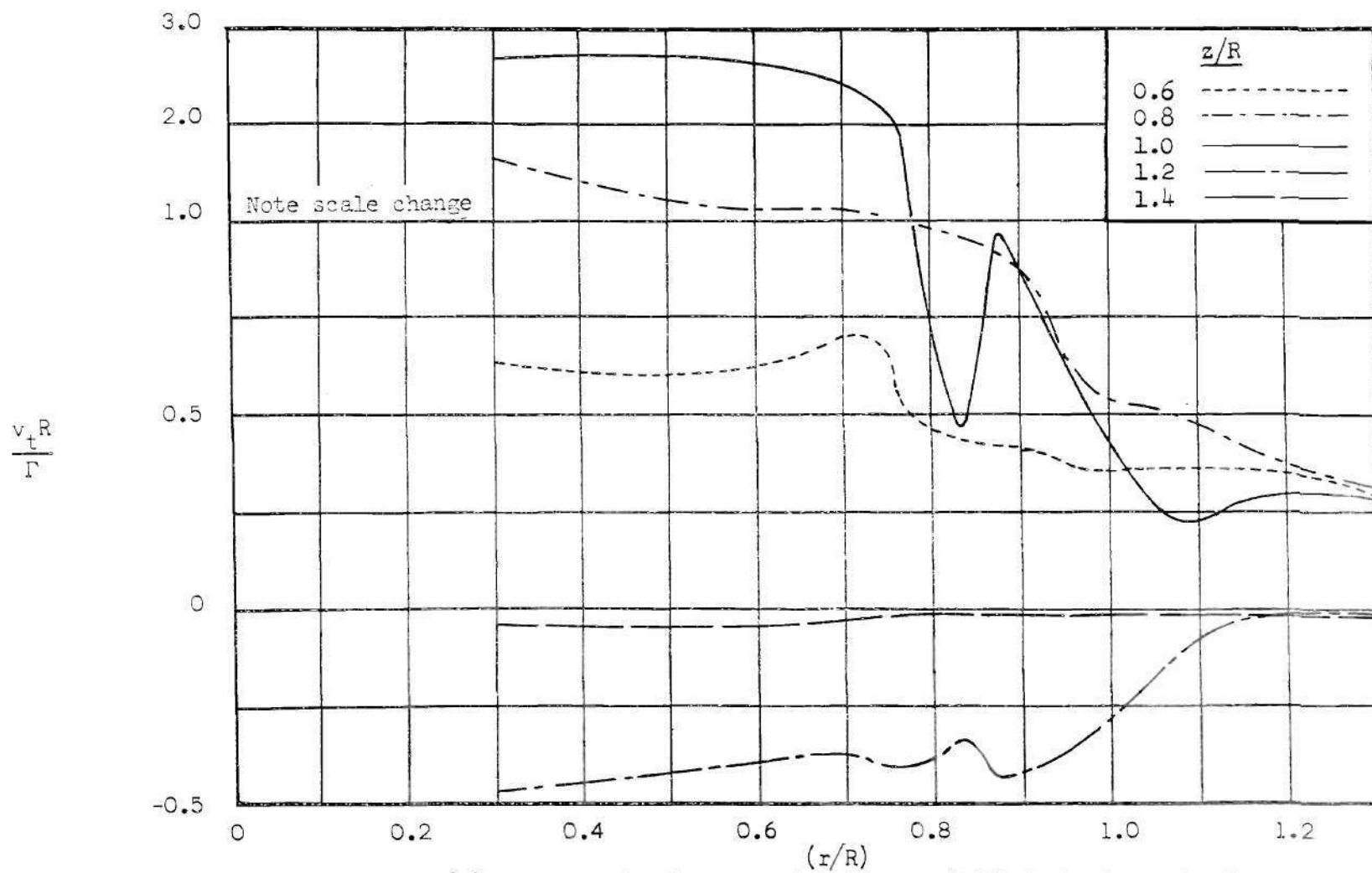
Figure 3. Search Coil Assembly



Figure 4. Normalizing Coil

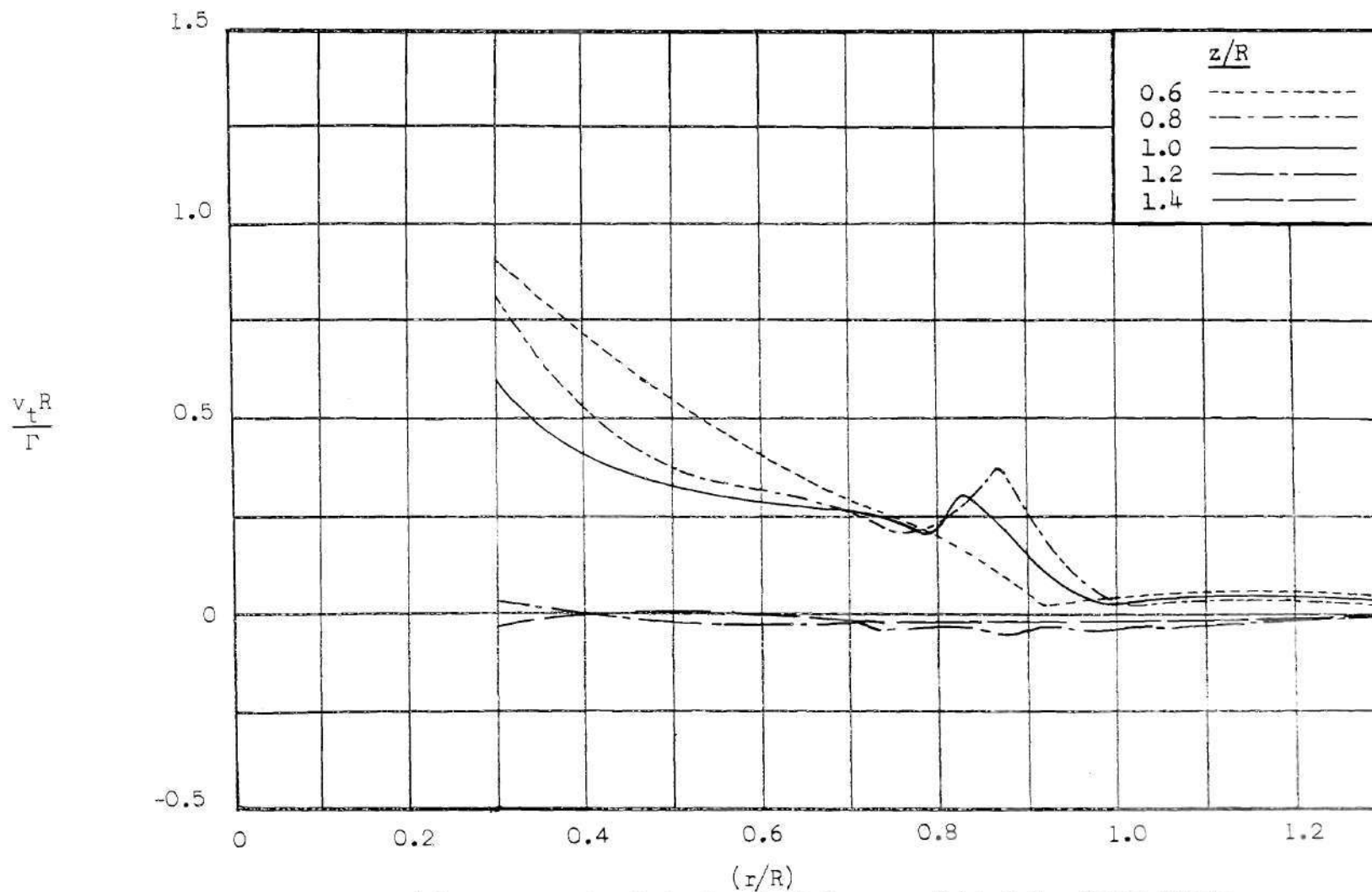


Figure 5. Amplifier and Output Meter



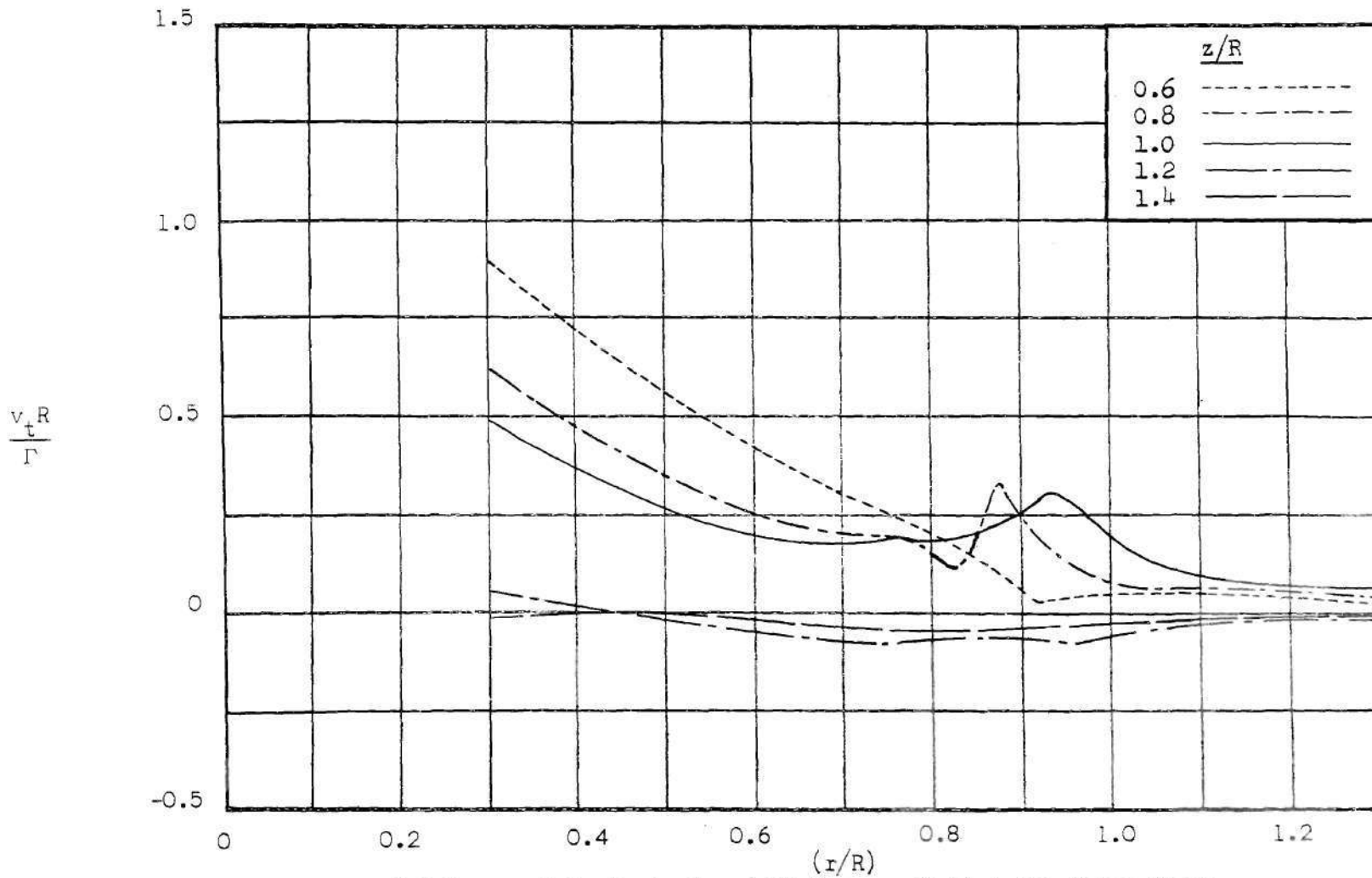
(a) For an Azimuth Angle of 5 Degrees Behind the Rotor Blade

Figure 6. Nondimensional Rotational Components of Induced Velocity at Various Nondimensional Heights



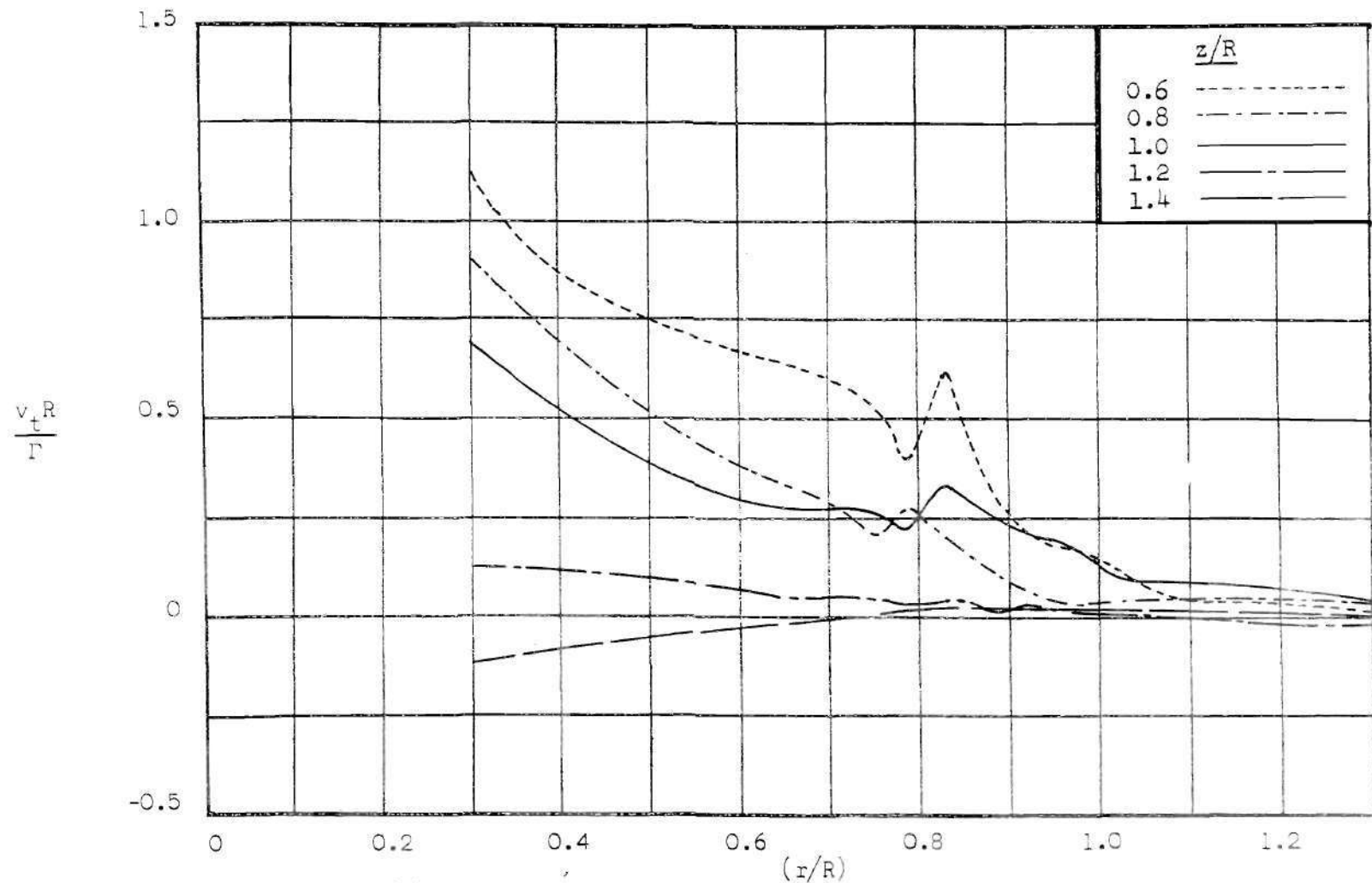
(b) For an Azimuth Angle of 50 Degrees Behind the Rotor Blade

Figure 6. Nondimensional Rotational Components of Induced Velocity at Various Nondimensional Heights (Continued)



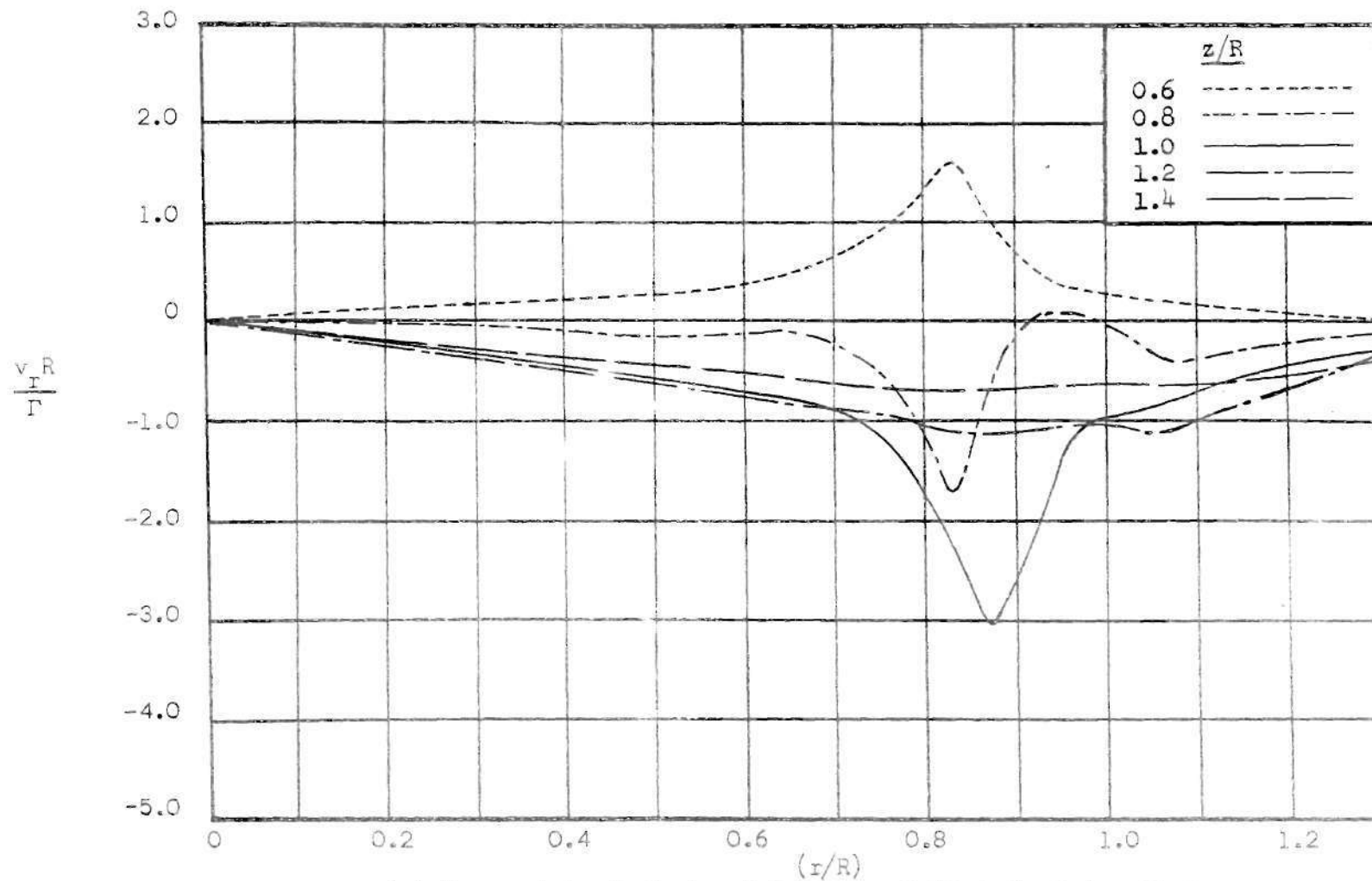
(c) For an Azimuth Angle of 95 Degrees Behind the Rotor Blade

Figure 6. Nondimensional Rotational Components of Induced Velocity at Various Nondimensional Heights (Continued)



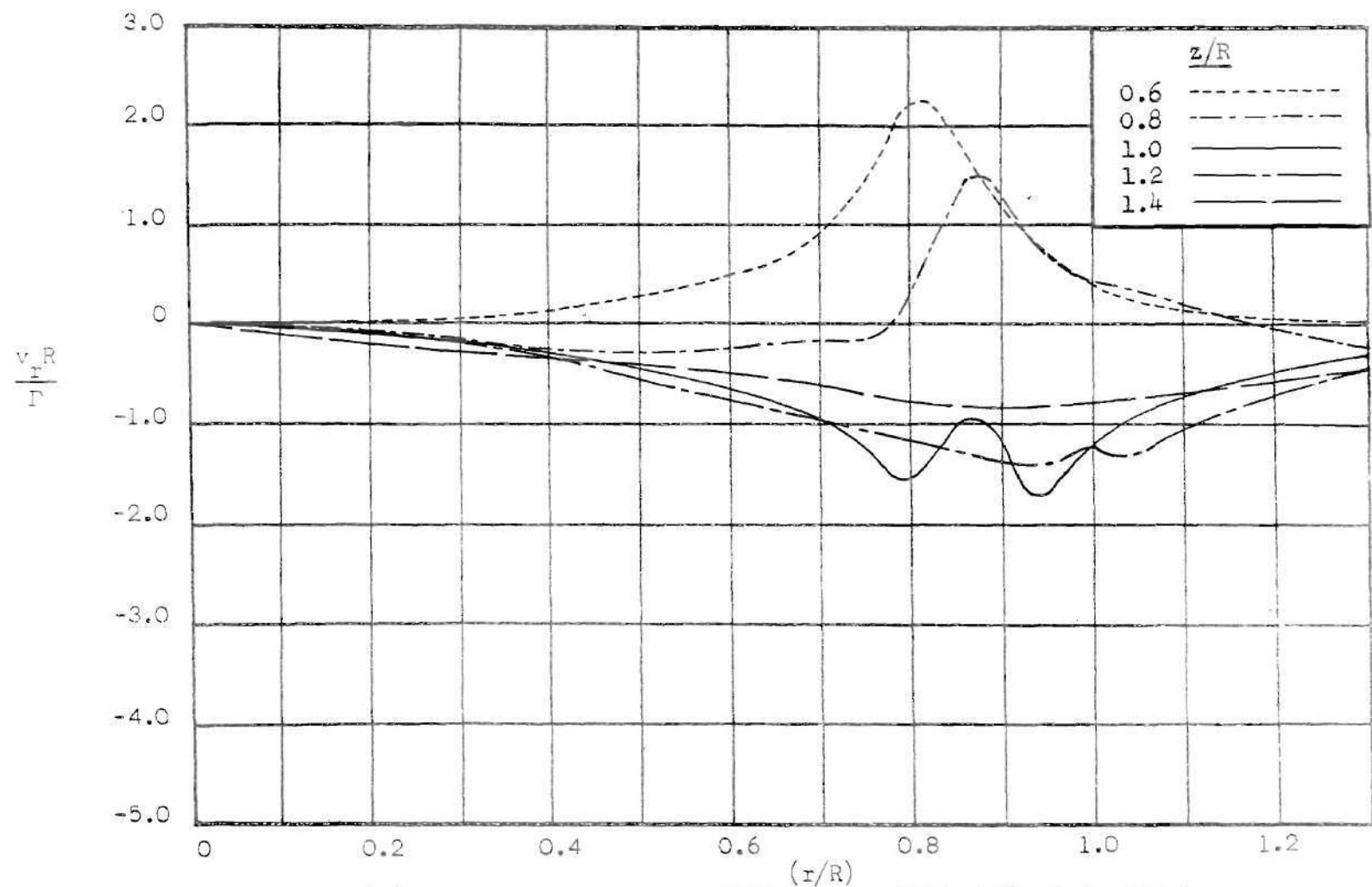
(d) For an Azimuth Angle of 140 Degrees Behind the Rotor Blade

Figure 6. Nondimensional Rotational Components of Induced Velocity at Various Nondimensional Heights (Continued)



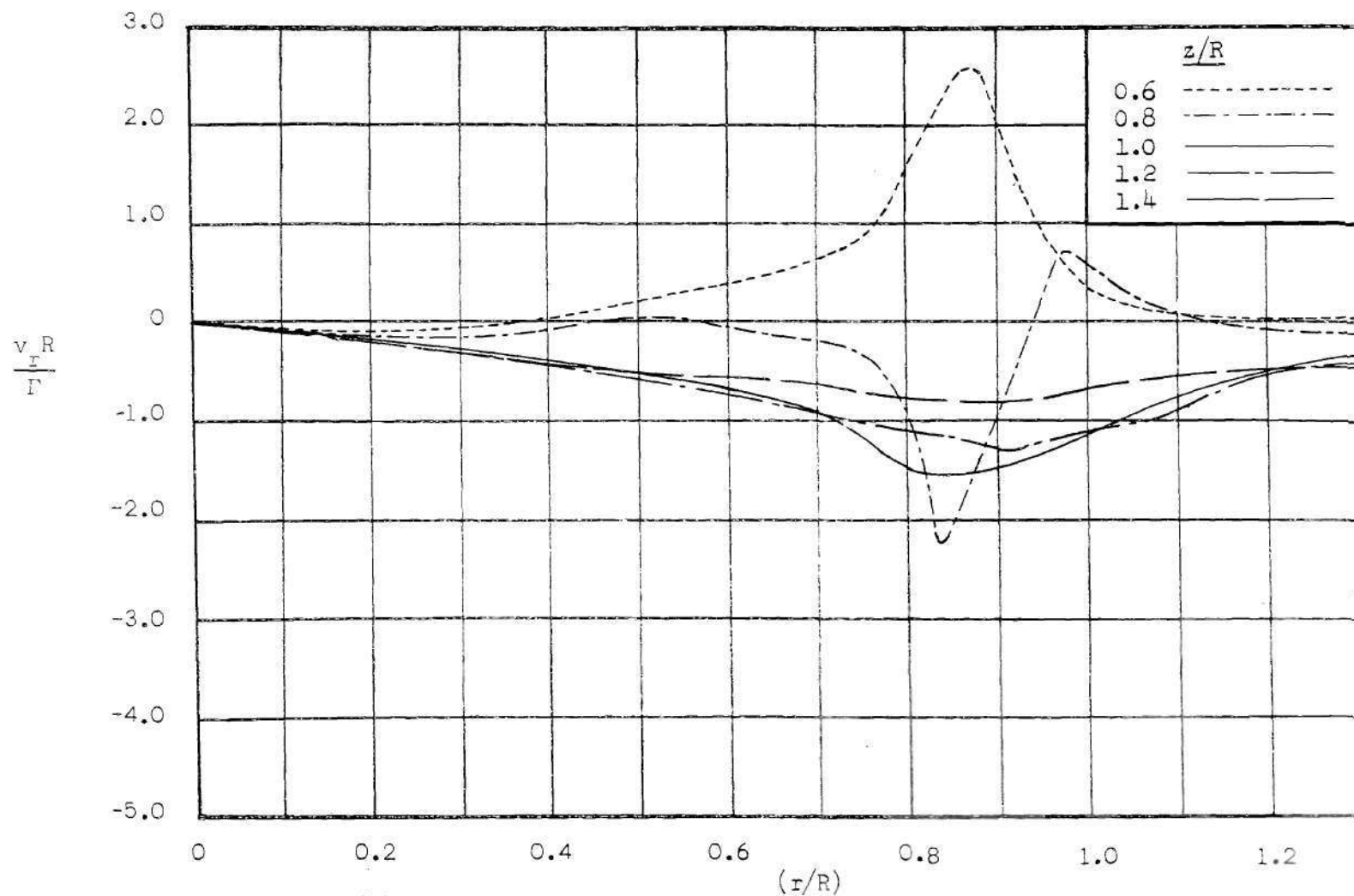
(a) For an Azimuth Angle of 5 Degrees Behind the Rotor Blade

Figure 7. Nondimensional Radial Components of Induced Velocity at Various Nondimensional Heights



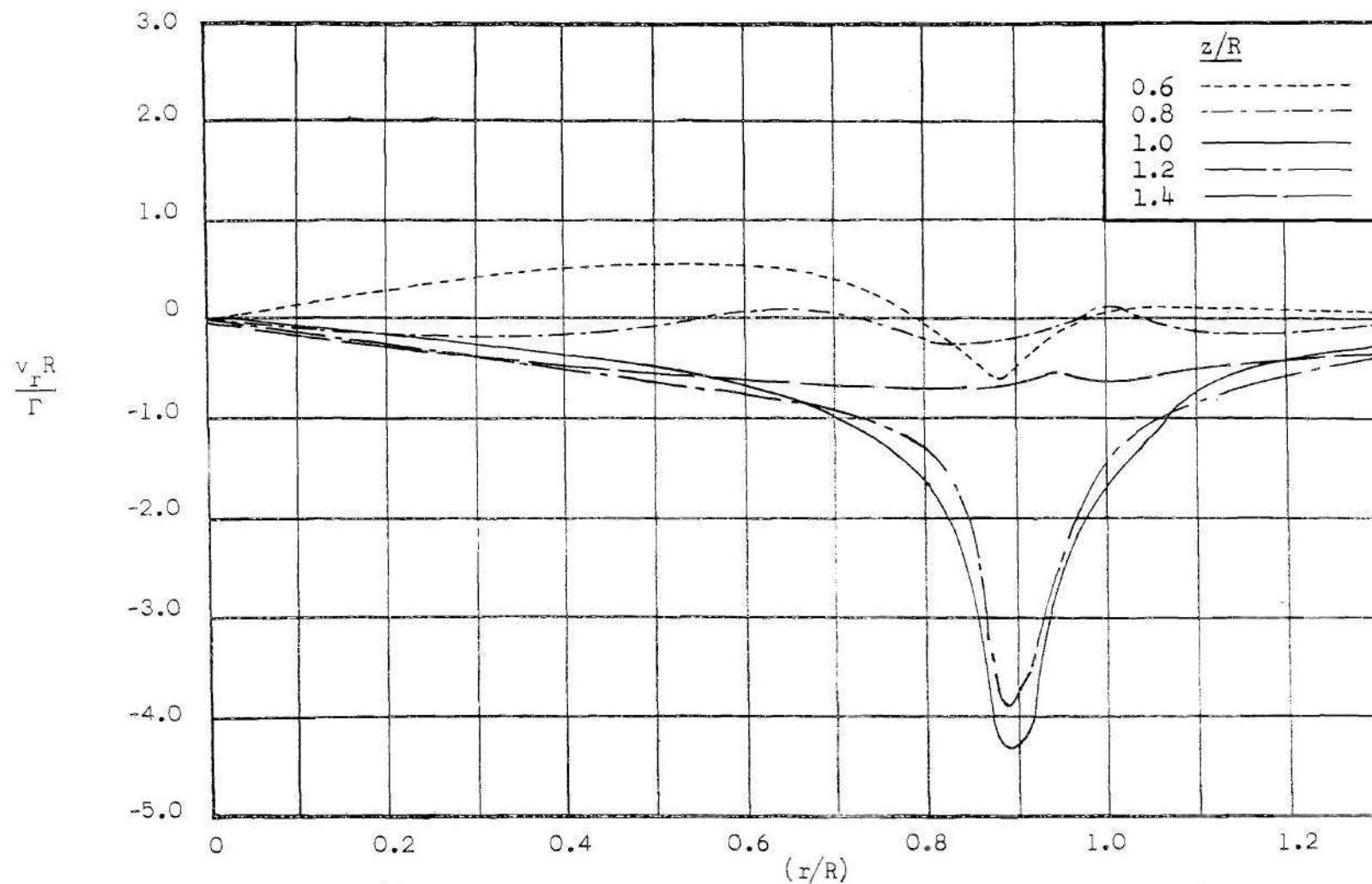
(b) For an Azimuth Angle of 50 Degrees Behind the Rotor Blade

Figure 7. Nondimensional Radial Components of Induced Velocity at Various Nondimensional Heights (Continued)



(c) For an Azimuth Angle of 95 Degrees Behind the Rotor Blade

Figure 7. Nondimensional Radial Components of Induced Velocity at Various Nondimensional Heights (Continued)



(d) For an Azimuth Angle of 140 Degrees Behind the Rotor Blade

Figure 7. Nondimensional Radial Components of Induced Velocity at Various Nondimensional Heights (Concluded)

BIBLIOGRAPHY

1. Gray, Robin B., An Experimental Smoke and Magnetic Analogy Study of the Induced Flow Field About a Model Rotor in Steady Flight Within Ground Effect, National Aeronautics and Space Administration Contract NAW 6520, August, 1959.
2. Castles, Walter, Jr., Durham, Howard L., Jr., and Kevorkian, Jirair, Normal Component of Induced Velocity For Entire Field of a Uniformly Loaded Lifting Rotor With Highly Swept Wake as Determined by Electromagnetic Analog, National Aeronautics and Space Administration, Technical Report R-41, 1959.